AGU PUBLICATIONS

Geophysical Research Letters

RESEARCH LETTER
10.1002/2016GL070524

Key Points:
- Geodynamic modeling results provide evidence for the former existence of large back-arc basins in the Neo-Tethys
- Comparisons to seismic tomography and the geoid show that standard reconstructions with purely northward dipping subduction are outdated
- The speed up of the Indian Plate at ~65 Ma may be due to a combination of a coupled double subduction zone system and plume push

Supporting Information:
- Supporting Information S1
- Data Set S1
- Data Set S2

Correspondence to:
R. Nerlich,
rnerlich@geophysik.uni-muenchen.de

Citation:
Nerlich, R., L. Colli, S. Ghelichkhan, B. Schuberth, and H.-P. Bunge (2016), Constraining central Neo-Tethys Ocean reconstructions with mantle convection models, *Geophys. Res. Lett.*, *43*, 9595–9603, doi:10.1002/2016GL070524.

Received 21 JUL 2016
Accepted 8 SEP 2016
Accepted article online 10 SEP 2016
Published online 29 SEP 2016

Constraining central Neo-Tethys Ocean reconstructions with mantle convection models

Rainer Nerlich[1], Lorenzo Colli[1], Siavash Ghelichkhan[1], Bernhard Schuberth[1], and Hans-Peter Bunge[1]

[1]Munich University, Department of Earth and Environmental Sciences (Geophysics), Munich, Germany

Abstract A striking feature of the Indian Ocean is a distinct geoid low south of India, pointing to a regionally anomalous mantle density structure. Equally prominent are rapid plate convergence rate variations between India and SE Asia, particularly in Late Cretaceous/Paleocene times. Both observations are linked to the central Neo-Tethys Ocean subduction history, for which competing scenarios have been proposed. Here we evaluate three alternative reconstructions by assimilating their associated time-dependent velocity fields in global high-resolution geodynamic Earth models, allowing us to predict the resulting seismic mantle heterogeneity and geoid signal. Our analysis reveals that a geoid low similar to the one observed develops naturally when a long-lived back-arc basin south of Eurasia's paleomargin is assumed. A quantitative comparison to seismic tomography further supports this model. In contrast, reconstructions assuming a single northward dipping subduction zone along Eurasia's margin or models incorporating a temporary southward dipping intraoceanic subduction zone cannot sufficiently reproduce geoid and seismic observations.

1. Introduction

1.1. The Central Neo-Tethys

The history of the ancient central Neo-Tethys Ocean, which ended in India-Eurasia collision and formation of the Himalayas, is difficult to constrain. Typically, one uses magnetic isochrones of the ocean floor to reconstruct ocean basins. But due to Neo-Tethys Ocean closure, these were lost to subduction, resulting in a lack of information on the basin's plate tectonic evolution. Based on indirect sources such as the interpretation of the local geology, mapping of ophiolites, and qualitative comparisons to seismic tomography, varying plate tectonic scenarios have been proposed [*Gibbons et al.*, 2015; *Hall*, 2012; *Metcalfe*, 1996; *Seton et al.*, 2012; *Stampfli and Borel*, 2002; *Van der Voo et al.*, 1999; *Zahirovic et al.*, 2012]. However, among these scenarios the number of subduction zones, their dip orientations, and their paleolocations differ substantially and remains controversial.

Currently, the Indian Ocean basin is characterized by one of Earth's most striking geoid lows extending from the tip of southern continental India beyond the equator to latitudes of >50°S (Figure 1, left). The Indian Ocean floor, moreover, records large convergence rate variations between India and Eurasia (Figure 1, right): A first temporary rate increase occurred ~90 Myr ago [*van Hinsbergen et al.*, 2011], but this observation has been challenged to reflect low-resolution effects from the employed rotations [*Eagles and Wibisono*, 2013]. The more prominent and unquestioned rate increase occurred ~70–65 Myr ago, followed by an equally strong decrease ~55–47 Myr ago [*Cande and Patriat*, 2015; *Copley et al.*, 2010; *Eagles and Wibisono*, 2013; *Gibbons et al.*, 2015; *Lee and Lawver*, 1995; *Molnar and Stock*, 2009; *Müller et al.*, 2016; *Patriat and Achache*, 1984; *Seton et al.*, 2012; *van Hinsbergen et al.*, 2011; *White and Lister*, 2012; *Zahirovic et al.*, 2012]. The trend is similar across different rotation models (Figure 1, right), although absolute values and timings are model dependent, owing to different interpretations and processing methods of magnetic data sets with variable data quality and source locations, and the use of different geological timescales [*Cande and Patriat*, 2015; *Seton et al.*, 2012]. The slowdown is generally attributed to a collisional event at the final stage of the Neo-Tethys Ocean closure, whose details remain debated [*Matthews et al.*, 2015]: Some argue for an immediate collision of (Greater) India with Eurasia [*Lee and Lawver*, 1995; *Patriat and Achache*, 1984], while others suggest preceding collisional events of either India with an intraoceanic arc [*Aitchison et al.*, 2007; *Bouilhol et al.*, 2013; *Gibbons et al.*, 2015; *Zahirovic et al.*, 2012] or Eurasia with a former microcontinent [*Van Hinsbergen et al.*, 2012]. Just as controversial are the underlying driving mechanisms for India's velocity variations: They have been linked to additional forcing from the arrival of mantle plumes [*Cande and Stegman*, 2011; *Eagles and*

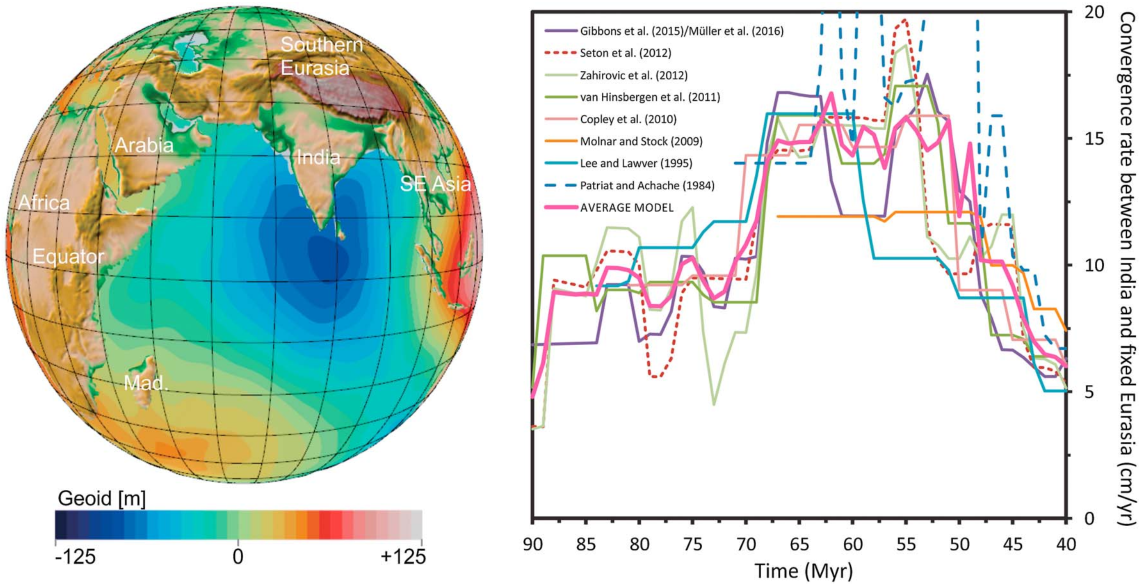

Figure 1. Observed (hydrostatic) geoid and India-Eurasia convergence rate variations. (left) One of Earth's most prominent geoid lows [*Pail et al*., 2010] is located south of continental India pointing to a regionally anomalous density distribution in the mantle beneath the ocean basin. (right) Reconstructed convergence rates between India and fixed Eurasia for a present-day reference point located at 28.5°N and 80°E showing a robust plate velocity peak between 70 and 50 Myr ago, despite large variations across different rotation models [*Copley et al*., 2010; *Gibbons et al*., 2015; *Lee and Lawver*, 1995; *Molnar and Stock*, 2009; *Müller et al*., 2016; *Patriat and Achache*, 1984; *Seton et al*., 2012; *van Hinsbergen et al*., 2011; *Zahirovic et al*., 2012]. Pink curve gives average convergence rate for the cited models.

Wibisono, 2013; *van Hinsbergen et al*., 2011], reduced frictional forces due to a thinned continental lithosphere beneath India in the wake of Gondwana breakup [*Kumar et al*., 2007], or most recently to a coupled double subduction zone system in front of the paleomargin of Eurasia [*Jagoutz et al*., 2015].

1.2. Plate Tectonic Scenarios

Mantle circulation models have long been recognized as powerful tools to distinguish competing plate tectonic scenarios [*Bunge and Grand*, 2000]. Thus, we test three reconstruction scenarios for the former central Neo-Tethys Ocean basin to explore geodynamic constraints on the subduction history of the central Neo-Tethys Ocean. The scenarios are made identical to each other (e.g., plate boundaries and reference frame) at the global scale, with the most recent global Earthbyte reconstructions [*Müller et al*., 2016] serving as base model, except for the assumed reconstruction scenarios in the Neo-Tethys/Indian Ocean realm. For the past 70 Myr, the base model links relative plate motions via Africa to a global moving hot spot reference frame [*Torsvik et al*., 2008], while a transitional reference frame—to minimize global net rotation and to ensure model smoothness—is used for the period between 70 and 105 Myr. For older times (>105 Myr) a true polar wander corrected reference frame was implemented [*Steinberger and Torsvik*, 2008].

The first scenario adopts the "standard" view of a single long-lived, northward dipping subduction zone beneath Eurasia (Figure 2a) [*Berra and Angiolini*, 2014; *Heine et al*., 2005; *Metcalfe*, 1996; *Seton et al*., 2012; *Torsvik et al*., 2010], to which we refer as the "*standard model*" (see supporting information).

The second scenario is the most recent unaltered global Earthbyte model [*Müller et al*., 2016], referred to as "Earthbyte 2016 model" (see supporting information for availability). It employs preexisting reconstructions for the Neo-Tethys Ocean [*Gibbons et al*., 2015] (Figure 2b), which were inspired by the regional geology and previous geodynamic modeling results [*Zahirovic et al*., 2012]. It contains an in series northward dipping subduction zone system for the central Neo-Tethys Ocean, consisting of a subduction zone along the paleo-margin of Eurasia and two temporary back-arc basins south of the continent's margin. The Kohistan-Ladakh back-arc basin opened 155 Myr ago and existed until 52 Myr, while the Woyla back-arc basin opened and closed between 145 Myr and 75 Myr ago, respectively.

We also explore a third scenario, named "alternative model" (Figure 2c) and motivated by the suggestion that high seismic velocity anomalies in the deep lower mantle beneath the southern Indian Ocean might originate

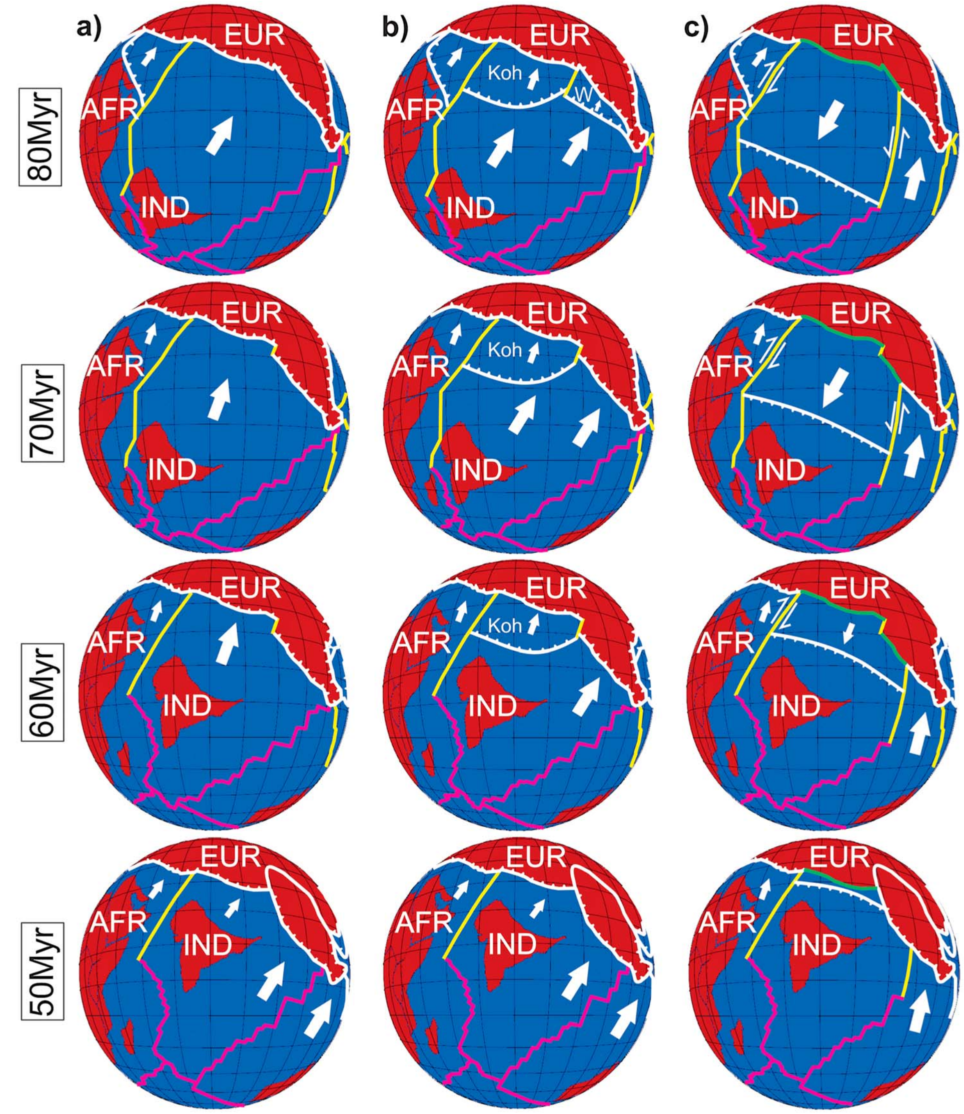

Figure 2. Three reconstructions for the Neo-Tethys Ocean (80–50 Myr). (a) The standard model assumes continuous northward dipping subduction beneath Eurasia, while (b) the Earthbyte 2016 reconstructions include back-arc basins south of Eurasia's paleomargin—the Woyla (W) and Kohistan-Ladakh (Koh) back-arc basins. (c) The alternative model assumes a temporarily passive Eurasian margin (indicated in green) and a southward dipping intraoceanic subduction zone north of India. As the extent of "Greater India" is debated [*Zahirovic et al.,* 2012], we show continental India's present-day geometry here. White arrows show schematically plate motion directions. Convergent/divergent/transform plate boundaries are shown in white/purple/yellow.

from a temporary southward dipping subduction zone [*Suppe et al*., 2014]. This unconventional scenario adjusts the standard model to contain a temporary northward retreating, southward dipping subduction zone for the time period 85–47 Myr, similar to a recently published reconstruction [*Hall*, 2012], but with a later timing of the subduction zone. The retreat velocity of the subduction hinge is determined by India's motion, resulting in a constant distance between the trench and India's continental margin. The model implies Eurasia to be a short-lived passive margin until the northward retreating subduction hinge impinges Eurasia's margin at 54 Myr, triggering a polarity reversal and resumption of northward dipping subduction, similar to preceding ideas [*Zahirovic et al*., 2012]. The polarity reversal occurs progressively from the eastern to the western edge of the central Neo-Tethys Ocean basin, which is bordered by large transform faults to the east and west (see supporting information).

2. Geodynamic Modeling

Our geodynamic modeling follows a standard approach [*Bunge et al*., 2002; *Schuberth et al*., 2009a] and makes use of the parallel mantle convection code TERRA [*Bunge et al*., 1997]. The grid point resolution is sufficiently high to simulate global mantle flow at Earth-like convective vigor (thermal Rayleigh number ~2×10^8). We assume a reference viscosity of 10^{21} Pa s in the asthenosphere (Figure S1), prescribe isothermal boundary conditions at the surface (300 K) and core mantle boundary (CMB, 4200 K), respectively, account for internal heating from radioactive decay, and implement a free-slip condition at the CMB (i.e., no shear stresses at this boundary) owing to the low viscosity of the core. At the surface we assimilate time-dependent velocity fields in accord with the three plate tectonic reconstruction scenarios described above. The latter is the only difference between the geodynamic simulations. The unknown initial condition of mantle heterogeneity required to start the simulations is approximated from global mantle flow assimilating the earliest (230 Myr) available plate configuration for 100 Myr, until a thermal quasi steady state is reached [*Bunge et al*., 2002; *Schuberth et al*., 2009a]. Further technical details on the model parameters are found in the supporting information and Table S1.

Time-dependent north-south profiles of the thermal mantle heterogeneity field at longitude 78°E from 90 to 50 Myr, the period containing India's fast northward motion, are shown in Figure 3 for all three simulations, with color reporting temperature variations relative to the mean layer temperatures. Figure 3a presents the standard model (Figure 2a). It shows an almost stationary northward dipping subduction zone (bluish colors indicate colder slab material) throughout that period along Eurasia's paleomargin. Figure 3b, based on the Earthbyte 2016 reconstructions (Figure 2a), shows the two northward dipping subduction zones located along the paleomargin of Eurasia and south of it in the intraoceanic realm. The basin between both subduction zones closes over time, eventually producing a single northward dipping subduction zone along Eurasia's paleomargin for times $<$52 Myr. Results from the alternative model (Figure 2c) are illustrated in Figure 3c. At 90 Myr, the model is identical to the standard model, because the intraoceanic southward subduction zone does not initiate until 85 Myr. The subduction hinge retreats quickly across the oceanic realm to the north in this model, particularly between 70 and 50 Myr, as prescribed by the assimilated plate motion.

A large thermal plume in the southern Neo-Tethys Ocean is present in all geodynamic models. It rises from the CMB and reaches the shallow mantle shortly before 80 Myr, entailing increased northward asthenosphere flow toward Eurasia until ~50 Myr. At the same time, there are remarkable differences in the subduction angle between the simulations. The standard and the Earthbyte 2016 models have steep dip angles of $>$45°, while the alternative model shows two distinct styles: Until ~70 Myr the dip angle is similar to the other models. But between ~70 and 50 Myr, the time corresponding to fast subduction hinge retreat, the dip angle is much shallower ($<$20°) producing a nearly flat slab in the shallow mantle beneath the Indian Ocean basin.

3. Comparison to Seismic Tomography and Observed Geoid

Tomographic filtering ensures a consistent comparison between our geodynamic simulations and seismic tomography model S40RTS [*Ritsema et al*., 2011; *Schuberth et al*., 2009b]. Thus, we convert the geodynamic temperature fields to seismic velocities, making use of a thermodynamically self-consistent mineralogical model [*Stixrude and Lithgow-Bertelloni*, 2011]. We also account for the long-wavelength character ($>$500 km) of the tomography model and the effects of heterogeneous data coverage and damping by filtering the seismic velocities tomographically with the resolution operator *R* that is exclusively published for S40RTS. Figure 4 shows transects through S40RTS (top) and our converted models with a midpoint centered on the equator at longitude 78°E and cutting through the approximate center of the observed Indian Ocean geoid low (Figure 1, left). In accord with other seismic tomography models [*Hafkenscheid et al*., 2006; *Simmons et al*., 2015; *Van der Voo et al*., 1999] S40RTS reveals a large positive (fast) seismic shear wave velocity anomaly —typically interpreted as subducted slab material—underneath India that extends south to a latitude of $>$35°S.

Our geodynamic simulation applying the standard model of a long-lived northward dipping subduction zone along Eurasia's paleomargin shows a prominent and nearly vertical high seismic velocity anomaly underneath India (Figure 4a), as expected. Positive anomalies in the lower mantle south of the equator are largely absent. The simulation based on the Earthbyte 2016 model in contrast shows high seismic velocity anomalies extending to far more southerly latitudes (Figure 4b), similar to the ones observed in S40RTS. The deepest

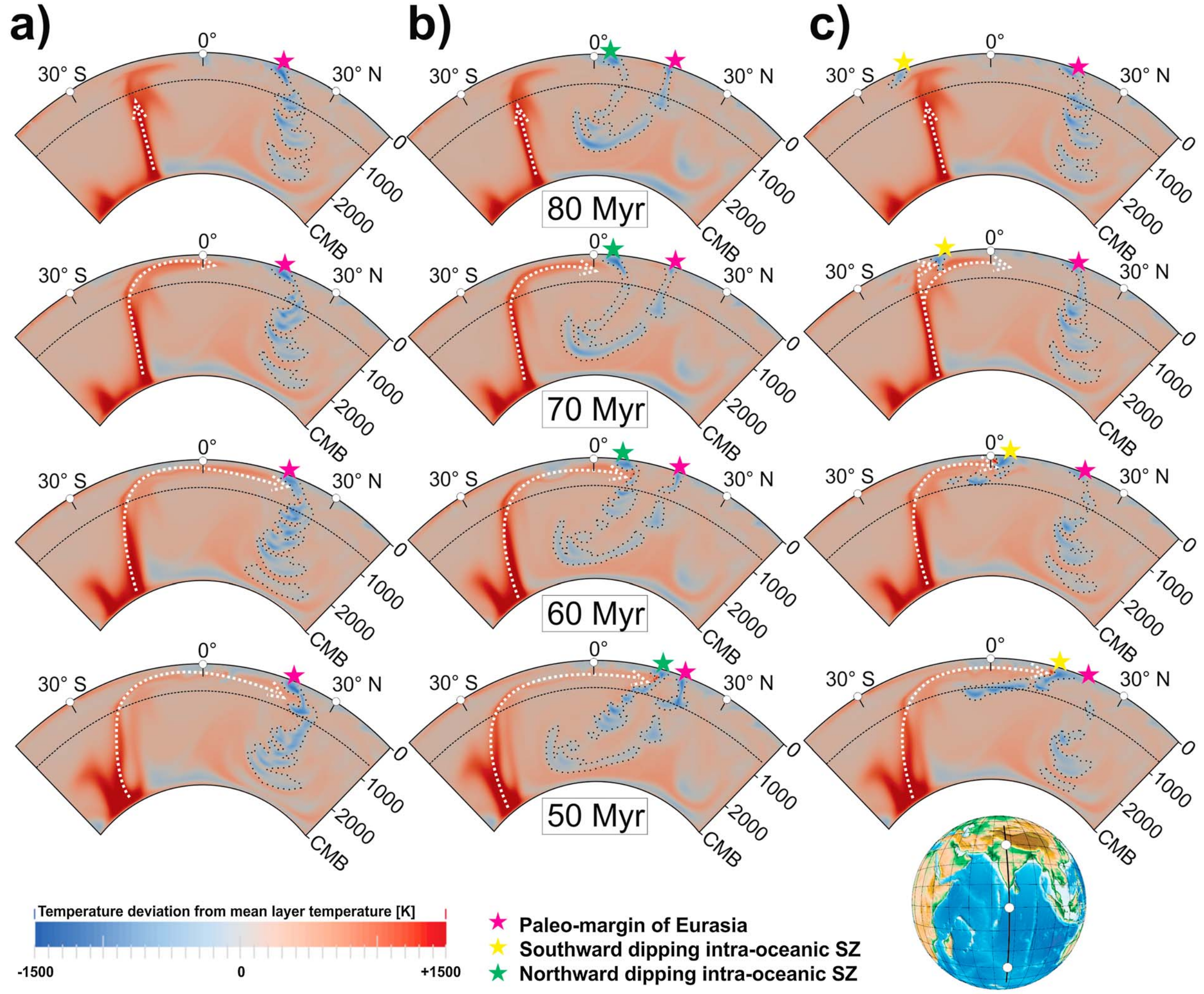

Figure 3. Cross sections through the geodynamic models. Temperature deviations from the mean layer temperatures based on (a) standard, (b) Earthbyte 2016, and (c) *alternative* reconstructions. Depth in km. Blue/red colors indicate colder/warmer regions; i.e., slabs have bluish colors and are outlined, while a mantle plume rising in the southern Neo-Tethys Ocean is characterized by deep reddish colors (emphasized with dotted arrows). Purple star locates paleomargin of Eurasia. Green star (model b) indicates location of the intraoceanic trench of the Kohistan-Ladakh back-arc basin. Yellow star (model c) represents the location of the northward retreating intraoceanic trench of the southward dipping subduction zone.

(2000 km, CMB) positive seismic velocities are observed at latitudes between ~30°S and ~21°S, becoming progressively shallower (~1500–2000 km) farther north between latitudes ~20°S and ~40°N. At the same time, slow seismic velocities are observed at shallower mantle depths between 400 and 1500 km. Some smaller-scale features present in S40RTS are not observed in the geodynamic simulation. But overall, the location and amplitude of heterogeneous structure are remarkably similar across the geodynamic and seismic models, even though the anomalies in S40RTS appear overall slightly broader. The alternative model (Figure 4c) shows fast seismic anomalies extending south of the equator to latitude ~20°S but remaining at shallow depth levels. Importantly, much of the equatorial mantle deeper than 1000 km is characterized by slow seismic velocities, in contrast to S40RTS.

The mineralogical model [*Stixrude and Lithgow-Bertelloni*, 2011] used to convert geodynamic to seismic heterogeneity also allows us to predict the mantle density distribution [*Schuberth et al.*, 2009b] and to compute synthetic geoids corresponding to the three different simulations for comparison with Earth's observed geoid (Figure 1, left) [*Pail et al.*, 2010]. Figure 5a illustrates the geoid signal implied by the standard reconstruction and the parameter choice of the geodynamic Earth model, with a geoid low located at the southernmost tip of continental India. Figure 5b reports the geoid predicted from the Earthbyte 2016 reconstructions. The geoid low in this case is placed farther south, as expected, and appears similar in location

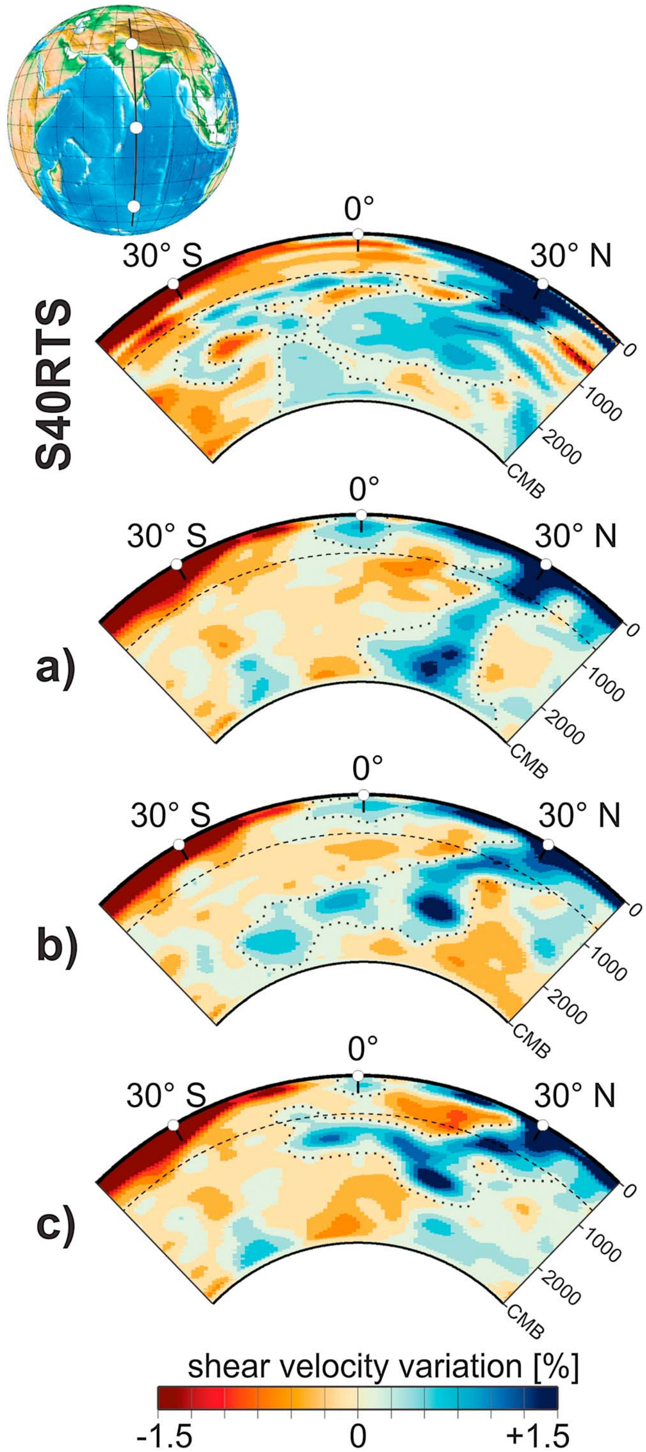

Figure 4. Comparison between S40RTS and geodynamic models. Cross sections at longitude 78°E through S40RTS (top) and the geodynamic models converted to seismic velocities with major high seismic velocity anomalies outlined. Profile location chosen to cut the approximate center of observed geoid low (Figure 1, left). Depth in km. (a) Standard model yields localized, almost vertical column of fast seismic anomalies near the India-Eurasia suture zone, while (b) the Earthbyte 2016 model and (c) the alternative model produce high seismic velocity anomalies south of the equator similar to those observed in S40RTS.

and amplitude to the observed geoid. The alternative reconstruction yields a regional geoid signal close to zero (Figure 5c) and compares unfavorable to the observed geoid.

4. Implications for Neo-Tethys Ocean Reconstructions

Our results are of great interest. They show that standard reconstructions of the central Neo-Tethys Ocean with a single long-lived, northward dipping subduction zone beneath Eurasia yield high seismic velocity slab material beneath present-day continental India as expected. Slabs south of the equator, as indicated tomographically, are absent and the geoid low is located farther north than observed, owing to the fact that the paleomargin of Eurasia remained north of the equator throughout the entire plate tectonic history—independent of the choice of reference frame [*Hafkenscheid et al.*, 2006; *Shephard et al.*, 2012; *Zahirovic et al.*, 2012].

The simulation based on the Earthbyte 2016 model shows high seismic velocity material up to 30° south of the equator even though the intraoceanic subduction zone assumed in this reconstruction remains close to the equator throughout the model's plate tectonic history. It predicts a geoid low similar in location to the observed one, which has been proposed to originate from high seismic velocity anomalies near the base of the mantle and low-velocity anomalies in the middle-to-upper mantle [*Spasojevic et al.*, 2010]. Thus, while the standard model is dominated by vertical slab sinking, the Earthbyte 2016 model is associated with substantial southward mantle flow. The disparity owes to age differences of the subducted material implied by the two reconstructions, because the back-arc basins of the Earthbyte 2016 model reduce the mean paleoseafloor age of the northern Neo-Tethys Ocean. For instance, at 65 Myr, the lithosphere descending along the Eurasian paleomargin in the standard reconstructions is

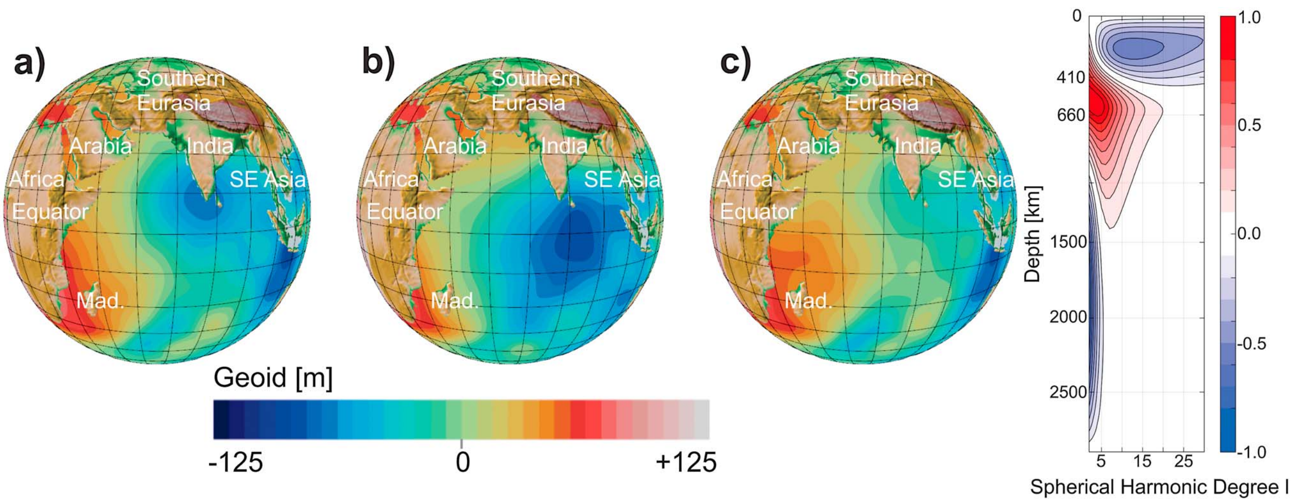

Figure 5. Predicted geoid signals for the three reconstruction scenarios. (a) Standard model yields localized geoid low at southern tip of continental India. (b) Geoid predicted from Earthbyte 2016 model is remarkably similar to the one observed (Figure 1, left), while (c) geoid signal associated with alternative model shows small negative values and is least comparable to observed geoid. Geoid kernel is shown on the right.

more than 40 Myr older than the one subducted along the in series double subduction zones of the Earthbyte 2016 model. Consequently, slab material associated with the latter reconstruction is entrained more easily by mantle wind of the deep Earth general circulation [*Tarduno et al.*, 2009], enabling southward transport of slab material by approximately 2000 km.

The alternative reconstructions yield a flat slab just below the upper/lower mantle transition (Figure 4c) and partially south of the equator, making this a viable model to deliver slab material far into the southern parts of the mantle beneath the Indian Ocean [*Suppe et al.*, 2014]. However, the slab remains at shallow depth levels, indicating slow sinking rates. The behavior is expected from numerical simulations showing that delayed slab descend into the deeper mantle is associated with subduction systems having high trench migration rates [*Christensen*, 1996]. Here the fast trench migration rate owes to India's rapid northward advance between 70 and 50 Myr (Figures 1 (right) and 3c).

The cause of India's rapid northward motion is difficult to understand, as the associated oceanic plate subduction is ultimately limited by the sinking of slab material into the lower mantle. Recently, it has been suggested that the number of subduction systems has a strong influence on plate migration rates and that an in series double subduction zone explains the observed convergence rate variations of India [*Jagoutz et al.*, 2015]. Moreover, the proximity in timing between India's speed up, a slowdown of Africa, and the coeval arrival of the Reunion plume, as evidenced by the Deccan Traps has been used to infer that the plume played a major role in accelerating India [*Cande and Stegman*, 2011; *Eagles and Wibisono*, 2013; *van Hinsbergen et al.*, 2011]. We note that all our models naturally develop a plume rising in the mantle beneath the southern Neo-Tethys Ocean from the CMB to Earth's surface. The latter increases the northward directed asthenosphere flow velocity beneath the Indian Plate by about a factor of 2 in our models (Figure 3). For our simulation with the Earthbyte 2016 reconstructions this leads to an intriguing timing: fast asthenosphere flow reaches the subducting slab of the intraoceanic subduction zone simultaneously with the onset of India's rapid plate convergence against Eurasia (Figure 1, right), literally pushing the cold descending slab northward (Figure 3b, at 70 Myr) until India slows down again (Figure 3b, at 50 Myr). This suggests that a combination of all proposed mechanisms may be responsible for India's rapid plate motion.

Our results show reconstructions that include large paleoback-arc basins in the central Neo-Tethys are suitable to explain the regional seismic and geoid observations. The arguments in favor of back-arc basins in the Neo-Tethys together with the existence of back-arc basins today suggest that they might be a more common feature throughout the Earth's plate tectonic history. An intriguing consequence from this would be a reduced mean paleoseafloor age [*Müller et al.*, 2016]. The latter affects buoyancy forces as well as slab sinking in the mantle and would potentially result in shallower mean paleo-ocean floor depths. Intraoceanic subduction related to back-arc basins may also account for high seismic velocity anomalies in the deep mantle, for example, those in the southwestern Pacific, which are otherwise hard to explain [*Schellart et al*., 2006]. Moreover, the currently accepted plate tectonic speed limits [*Schult and Gordon*, 1984] might temporarily be overcome if double subduction zone systems were more common in the plate tectonic record. Future tests for other intraoceanic back-arc basins in the plate tectonic record should involve the use of global geodynamic models in conjunction with seismic, gravity, and other geological observations.

Acknowledgments
For permission to present some of the figures in this paper using 4DPlates, we thank Statoil and Kalkulo A.S. Further, we thank Editor Jeroen Ritsema and two anonymous reviewers for their constructive comments. R.N., L.C., S.G., and H.P.B. acknowledge funding from the DFG priority program SPP 1375-SAMPLE. All data for this paper are properly cited and referred to in the reference list or may be found in the supporting information.

References

Aitchison, J. C., J. R. Ali, and A. M. Davis (2007), When and where did India and Asia collide?, *J. Geophys. Res.*, *112*, B05423, doi:10.1029/2006JB004706.

Berra, F., and L. Angiolini (2014), The evolution of the Tethys region throughout the Phanerozoic: A brief tectonic reconstruction, in *Petroleum Systems of the Tethyan Region*, edited by L. Marlow, C. Kendall, and L. Yose, *AAPG Mem.*, 106, pp. 1–27, doi:10.1306/13431840m1063606.

Bouilhol, P., O. Jagoutz, J. M. Hanchar, and F. O. Dudas (2013), Dating the India–Eurasia collision through arc magmatic records, *Earth Planet. Sci. Lett.*, *366*, 163–175, doi:10.1016/j.epsl.2013.01.023.

Bunge, H.-P., and S. P. Grand (2000), Mesozoic plate-motion history below the northeast Pacific Ocean from seismic images of the subducted Farallon slab, *Nature*, *405*, 337–340, doi:10.1038/35012586.

Bunge, H.-P., M. A. Richards, and J. R. Baumgardner (1997), A sensitivity study of 3-D-spherical mantle convection at 10^8 Rayleigh number: Effects of depth-dependent viscosity, heating mode and an endothermic phase change, *J. Geophys. Res.*, *102*, 11,991–12,007, doi:10.1029/96JB03806.

Bunge, H.-P., M. A. Richards, and J. R. Baumgardner (2002), Mantle circulation models with sequential data-assimilation: Inferring present-day mantle structure from plate motion histories, *Phil. Trans. R. Soc. London, Ser. A*, *360*, 2545–2567, doi:10.1098/rsta.2002.1080.

Cande, S. C., and P. Patriat (2015), The anticorrelated velocities of Africa and India in the Late Cretaceous and early Cenozoic, *Geophys. J. Int.*, *200*, 227–243, doi:10.1093/gji/ggu392.

Cande, S. C., and D. R. Stegman (2011), Indian and African plate motions driven by the push force of the Réunion plume head, *Nature*, *475*, 47–52, doi:10.1038/nature10174.

Christensen, U. R. (1996), The influence of trench migration on slab penetration into the lower mantle, *Earth Planet. Sci. Lett.*, *140*, 27–39, doi:10.1016/0012-821X(96)00023-4.

Copley, A., J.-P. Avouac, and J.-Y. Royer (2010), India-Asia collision and the Cenozoic slowdown of the Indian Plate: Implications for the forces driving plate motions, *J. Geophys. Res.*, *115*, B03410, doi:10.1029/2009JB006634.

Eagles, G., and A. D. Wibisono (2013), Ridge push, mantle plumes and the speed of the Indian Plate, *Geophys. J. Int.*, *194*(2), 670–677, doi:10.1093/gji/ggt162.

Gibbons, A. D., S. Zahirovic, R. D. Müller, J. Whittaker, and V. Yatheesh (2015), A tectonic model reconciling evidence for the collisions between India, Eurasia and intra-oceanic arcs of the central-eastern Tethys, *Gondwana Res.*, *28*, 451–492, doi:10.1016/j.gr.2015.01.001.

Hafkenscheid, E., M. J. R. Wortel, and W. Spakman (2006), Subduction history of the Tethyan region derived from seismic tomography and tectonic reconstructions, *J. Geophys. Res.*, *111*, B08401, doi:10.1029/2005JB003791.

Hall, R. (2012), Late Jurassic–Cenozoic reconstructions of the Indonesian region and the Indian Ocean, *Tectonophysics*, *570–571*, 1–41, doi:10.1016/j.tecto.2012.04.021.

Heine, C., R. D. Müller, and C. Gaina (2005), Reconstructing the lost eastern Tethys Ocean basin: Convergence history of the SE Asian margin and marine gateways, *Geophysical Monogr. Ser.*, *149*, 37–54, doi:10.1029/149GM03.

Jagoutz, O., L. Royden, A. F. Holt, and T. W. Becker (2015), Anomalously fast convergence of India and Eurasia caused by double subduction, *Nat. Geosci.*, *8*, 475–479, doi:10.1038/ngeo2418.

Kumar, P., X. Yuan, M. R. Kumar, R. Kind, X. Li, and R. K. Chadha (2007), The rapid drift of the Indian tectonic plate, *Nature*, *449*, 894–897, doi:10.1038/nature06214.

Lee, T.-Y., and L. A. Lawver (1995), Cenozoic plate reconstruction of Southeast Asia, *Tectonophysics*, *251*, 85–138, doi:10.1016/0040-1951(95)00023-2.

Matthews, K. J., R. D. Müller, and D. T. Sandwell (2015), Oceanic microplate formation records the onset of India–Eurasia collision, *Earth Planet. Sci. Lett.*, *433*, 204–214, doi:10.1016/j.epsl.2015.10.040.

Metcalfe, I. (1996), Gondwanaland dispersion, Asian accretion and evolution of eastern Tethys, *Aust. J. Earth Sci.*, *43*, 605–623, doi:10.1016/j.jseaes.2012.12.020.

Molnar, P., and J. M. Stock (2009), Slowing of India's convergence with Eurasia since 20 Ma and its implications for Tibetan mantle dynamics, *Tectonics*, *28*, TC3001, doi:10.1029/2008TC002271.

Müller, R. D., et al. (2016), Ocean basin evolution and global-scale plate reorganization events since Pangea breakup, *Annu. Rev. Earth Planet. Sci.*, *44*(1), 107–138, doi:10.1146/annurev-earth-060115-012211.

Pail, R., et al. (2010), Combined satellite gravity field model GOCO01S derived from GOCE and GRACE, *Geophys. Res. Lett.*, *37*, L20314, doi:10.1029/2010GL044906.

Patriat, P., and J. Achache (1984), India-Eurasia collision chronology has implications for crustal shortening and driving mechanism of plates, *Nature*, *311*, 615–621, doi:10.1038/311615a0.

Ritsema, J., H. J. van Heijst, A. Deuss, and J. H. Woodhouse (2011), S40RTS: A degree-40 shear-velocity model for the mantle from new Rayleigh wave dispersion, teleseismic traveltimes, and normal-mode splitting function measurements, *Geophys. J. Int.*, *184*, 1223–1236, doi:10.1111/j.1365-246X.2010.04884.x.

Schellart, W. P., G. S. Lister, and V. G. Toy (2006), A Late Cretaceous and Cenozoic reconstruction of the Southwest Pacific region: Tectonics controlled by subduction and slab rollback processes, *Earth Sci. Rev.*, *76*, 191–233, doi:10.1016/j.earscirev.2006.01.002.

Schuberth, B. S. A., H.-P. Bunge, G. Steinle-Neumann, C. Moder, and J. Oeser (2009a), Thermal versus elastic heterogeneity in high-resolution mantle circulation models with pyrolite composition: High plume excess temperatures in the lowermost mantle, *Geochem. Geophys. Geosyst.*, *10*, Q01W01, doi:10.1029/2008GC002235.

Schuberth, B. S. A., H.-P. Bunge, and J. Ritsema (2009b), Tomographic filtering of high-resolution mantle circulation models: Can seismic heterogeneity be explained by temperature alone?, *Geochem. Geophys. Geosyst.*, *10*, Q05W03, doi:10.1029/2009GC002401.

Schult, F. R., and R. G. Gordon (1984), Root mean square velocities of the continents with respect to the hot spots since the Early Jurassic, *J. Geophys. Res.*, *89*, 1789–1800, doi:10.1029/JB089iB03p01789.

Seton, M., et al. (2012), Global continental and ocean basin reconstructions since 200 Ma, *Earth Sci. Rev.*, *113*, 212–270, doi:10.1016/j.earscirev.2012.03.002.

Shephard, G. E., H.-P. Bunge, B. S. A. Schuberth, R. D. Müller, A. S. Talsma, C. Moder, and T. Landgrebe (2012), Testing absolute plate reference frames and the implications for the generation of geodynamic mantle heterogeneity structure, *Earth Planet. Sci. Lett.*, *317–318*, 204–217, doi:10.1016/j.epsl.2011.11.027.

Simmons, N. A., S. C. Myers, E. Johannesson, E. Matzel, and S. P. Grand (2015), Evidence for long-lived subduction of an ancient tectonic plate beneath the southern Indian Ocean, *Geophys. Res. Lett.*, *42*, 9270–9278, doi:10.1002/2015GL066237.

Spasojevic, S., M. Gurnis, and R. Sutherland (2010), Mantle upwellings above slab graveyards linked to the global geoid lows, *Nat. Geosci.*, *3*, 435–438, doi:10.1038/ngeo855.

Stampfli, G. M., and G. D. Borel (2002), A plate tectonic model for the Paleozoic and Mesozoic constrained by dynamic plate boundaries and restored synthetic oceanic isochrons, *Earth Planet. Sci. Lett.*, *196*, 17–33, doi:10.1016/S0012-821X(01)00588-X.

Steinberger, B., and T. H. Torsvik (2008), Absolute plate motions and true polar wander in the absence of hotspot tracks, *Nature*, *452*, 620–623, doi:10.1029/2007RG000227.

Stixrude, L., and C. Lithgow-Bertelloni (2011), Thermodynamics of mantle minerals—II. Phase equilibria, *Geophys. J. Int.*, *184*, 1180–1213, doi:10.1111/j.1365-246X.2010.04890.x.

Suppe, J., J. Wu, C. D. J. Lin, and V. S. Kanda (2014), The trajectory of India towards Eurasia recorded by subducted slabs: Evidence for southward subduction of the Tethys Ocean under India after 130 Ma, paper presented at Geophysical Research Abstracts - EGU General Assembly (2014), Vienna.

Tarduno, J., H.-P. Bunge, N. Sleep, and U. Hansen (2009), The bent Hawaiian-Emperor hotspot track: Inheriting the mantle wind, *Science*, *324*, 50–53, doi:10.1126/science.1161256.

Torsvik, T. H., B. Steinberger, M. Gurnis, and C. Gaina (2010), Plate tectonics and net lithosphere rotation over the past 150 My, *Earth Planet. Sci. Lett.*, *291*, 106–112, doi:10.1016/j.epsl.2009.12.055.

Torsvik, T. H., R. D. Müller, R. Van der Voo, B. Steinberger, and C. Gaina (2008), Global plate motion frames: Toward a unified model, *Rev. Geophys.*, *46*, RG3004, doi:10.1029/2007RG000227.

Van der Voo, R., W. Spakman, and H. Bijwaard (1999), Tethyan subducted slabs under India, *Earth Planet. Sci. Lett.*, *171*, 7–20, doi:10.1016/S0012-821X(99)00131-4.

van Hinsbergen, D. J. J., B. Steinberger, P. V. Doubrovine, and R. Gassmöller (2011), Acceleration and deceleration of India-Asia convergence since the Cretaceous: Roles of mantle plumes and continental collision, *J. Geophys. Res.*, *116*, B06101, doi:10.1029/2010JB008051.

Van Hinsbergen, D. J. J., P. C. Lippert, G. Dupont-Nivet, N. McQuarrie, P. V. Doubrovine, W. Spakman, and T. Torsvik (2012), Greater India Basin hypothesis and a two-stage Cenozoic collision between India and Asia, *Proc. Natl. Acad. Sci. U.S.A.*, *109*, 7659–7664, doi:10.1073/pnas.1117262109.

White, L. T., and G. S. Lister (2012), The collision of India with Asia, *J. Geodyn.*, *56–57*, 7–17, doi:10.1016/j.jog.2011.06.006.

Zahirovic, S., R. D. Müller, M. Seton, N. Flament, M. Gurnis, and J. Whittaker (2012), Insights on the kinematics of the India-Eurasia collision from global geodynamic models, *Geochem. Geophys. Geosyst.*, *13*, Q04W11, doi:10.1029/2011GC003883.